THE JOURNAL OF PHYSICAL CHEMISTRY C

Article

pubs.acs.org/JPCC

Stability and Hydrogen Affinity of Graphite-Supported Wires of Cu, Ag, Au, Ni, Pd, and Pt

Germán J. Soldano,*[,†,∥] Paola Quaino,[†,‡] Elizabeth Santos,[†,§] and Wolfgang Schmickler[†]

[†]Institute of Theoretical Chemistry, Ulm University, D-89069 Ulm, Germany

[‡]PRELINE, Universidad Nacional del Litoral, 3000 Santa Fé, Argentina

[§]Facultad de Matemáticas, Astronomía y Física, Universidad Nacional de Córdoba, 5000 Córdoba, Argentina

ABSTRACT: The stability of Cu, Ag, Au, Ni, Pd, and Pt nanowires supported on graphite steps is investigated by density functional theory. Two step borders are examined: armchair and zigzag. It was found that the Ni, Pd, and Pt wires are more stable than coinage metal ones and that the zigzag configuration is the most energetically favored. The adsorption of hydrogen on such systems is also studied. In Ni, Pd, and Pt graphite-supported wires the reaction occurs on the wire, while in coinage metal wires hydrogen adsorbs directly on graphite steps, breaking the bond between wire and step. Our results suggest that, in early stages of wire formation, hydrogen adsorption could induce the desorption of coinage metals from graphite. The catalytic properties for hydrogen adsorption on graphite-supported and freestanding nanowires are also compared.

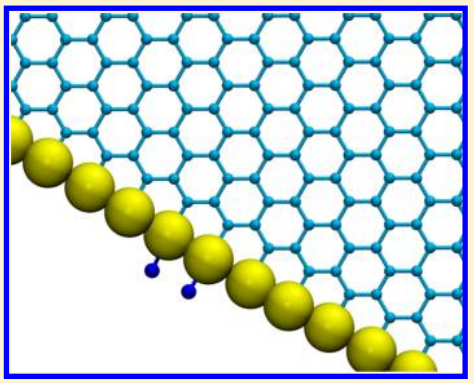

INTRODUCTION

Metal nanowires have many applications in nanotechnology: as chemical sensors,[1−6] for nanoelectronics, as superstrong and tough composites, in functional nanostructured materials, and for novel probe microscopy tips.[7] From the electrochemical point of view, these wires are interesting due to their unique electronic structure: the *density of states* (DOS) of nanowires shows substantial d band upshifts in comparison with the DOS of fcc(111) surfaces, particularly for Cu and Au. As predicted by the d band model,[8,9] these upshifts make Cu and Au wires excellent catalysts for the hydrogen evolution reaction (HER).[10]

However, in order to be used as catalysts in real devices, such wires need to be supported on inert substrates. Promising systems are wires adsorbed at the edge of graphite steps, which are obtained by *electrochemical step edge decoration*.[11] These so-called graphite-supported wires (GSWs) are stable even above 600 K.[12,13] In such structures, graphite steps are first oxidized, then metal clusters nucleate at the steps, and finally, these particles grow to coalescence into continuous metal wires.

Another possibility is to support the wires on graphene, which are isolated graphite single layers. Several experimental techniques are given in the references for fabricating such structures, among which we mention lithographic patterning,[14−17] sonochemical methods,[18,19] and carbon nanotube unzipping by metallic nanoparticles.[20−25] Graphene itself exhibits interesting optical, thermal, mechanical, and electronic properties,[26−28] such as high electron mobility at room temperature and a band gap between 0.5 and 3.0 eV depending on the graphene width. For an extended review on graphene, we recommend Acik and Chabal.[29] Concerning the chemical reactivity of both graphite and graphene, it is clear that the edges are more reactive than the perfectly bonded sp carbon atoms in the basal plane. In fact, it was found that atomic layer deposition of metal oxide occurs only if the pristine graphene surface is functionalized or presents dangling bonds.[30] Similarly, experiments and theory show that there is no electron-induced interaction between Cr clusters and pristine graphene.[31]

A major challenge in the fabrication of these devices is to control the structure and functionalization at the edges. Details concerning the structure of the nucleation seeds are difficult to explore, given the large diversity of possible configurations. The systematic exploration of several structures by means of density functional theory helps in selecting those configurations of relative importance as well as in eliminating those with energetic instability. Thus, even if the most stable structure is not found, this theoretical study *restricts* the search, guiding the work of experimentalists.

We shall treat here the hypothetical scenario of direct bond formation between the metal and the graphite step. This has been experimentally observed for the case of Cr at the zigzag edges of graphene.[31] We leave the cases of oxygen structures for a future study. In a previous work we have investigated Pt and Au wires at the zigzag edge of graphite sheets.[32] In this work we extend our study to six metals (Ni, Pd, Pt, Cu, Ag, and Au) forming wires at the two stable graphite step edges: zigzag and armchair steps (see Figures 1 and 2). The catalytic properties for hydrogen oxidation are also investigated.

We shall also compare these results with those of the freestanding wires, which are promising catalysts. The stability

Received: June 27, 2013
Revised: August 7, 2013
Published: August 26, 2013

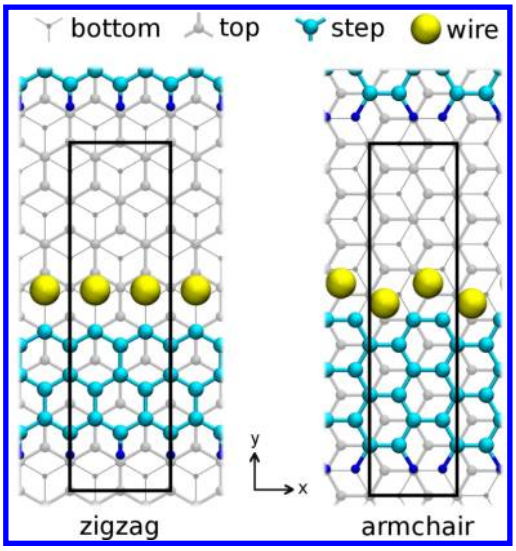

Figure 1. Lateral unit cell of zigzag and armchair graphite-supported wires. The lateral unit cell is sketched with black plain lines.

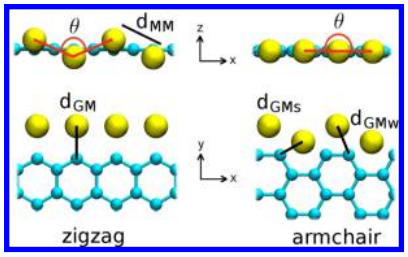

Figure 2. Relevant distances and angles of armchair and zigzag GSWs.

of supported wires at high temperatures suggests a strong graphite−wire interaction. If that is the case, is graphite only a supporting media for the nanowires or does it modify their unique chemical properties?

This work is organized as follows: First the metal−step bond is studied and discussed in detail. Then the affinity of hydrogen to the wire and to the graphite step (leading in some cases to wire desorption) is compared. Later, the kinetics of hydrogen adsorption and oxidation in an electrochemical environment are explored. Finally, the results of this work are summarized in the Conclusions.

RESULTS

Characterization and Stability. As one can observe in Figure 1, the distances from the metal atoms to the step are the same for the zigzag edges. In contrast, for the armchair case, there are two nonequivalent metal atoms. One is surrounded by four nearest neighbors, and is strongly adsorbed to the step (M_s). The other is surrounded by two nearest neighbors, and is weakly adsorbed to the step (M_w). The corresponding distances are d_{GM_w} and d_{GM_s}. The graphite−wire distances for zizag (d_{GM}) and armchair (d_{GM_s} and d_{GM_w}) GSWs are depicted in Figure 2 and summarized in Table 1. The step of armchair GSWs is perfectly planar, while the metal wires at zigzag GSWs show a corrugation along the z axis forming an angle θ as indicated in Figure 2. Since the metal atoms in the armchair-supported wires are not all equivalent, a similar corrugation is observed in the xy plane.

Due to the graphite lattice, the closest metal−metal distance (d_{MM}) of zigzag GSWs is 2.46 Å, which corresponds to a

Table 1. Values of Distances and Angles Shown in Figure 2[a]

	Ni	Pd	Pt	Cu	Ag	Au
d_{GM}(zz) [Å]	1.80	1.97	1.94	1.92	2.14	2.08
d_{GM_s}(arm) [Å]	1.93	2.06	2.07	1.96	2.13	2.10
d_{GM_w}(arm) [Å]	2.03	3.05	3.05	2.30	3.38	3.29
d_{MM}(NW) [Å]	2.13	2.50	2.39	2.32	2.64	2.61
θ(zz) [deg]	180	145	151	180	132	134
θ(arm) [deg]	180	180	180	180	180	180

[a]The wire−bond distance (d_{MM}) is compared with that of bare wires (NWs). "zz" corresponds to zigzag and "arm" to armchair.

noncorrugated wire. If d_{MM} of bare wires is smaller than this value, the corresponding supported wires will have no corrugation; otherwise, the bigger d_{MM} of the bare wires is, the more corrugated will be the supported wire ($\theta < 180°$).

The configuration of metal wires at the zigzag edges is in agreement with experimental and theoretical results of Wang et al.[31] The authors also found that, for small Cr and Pt clusters, there is a tendency to assemble in line instead of in configurations of larger dimensions.

The binding energy between graphite and wire (E_b) for armchair and zigzag is calculated according to eq 1:

$$E_b = (E_G + E_{NW} - E_{GSW})/m \quad (1)$$

where E_{GSW}, E_G, and E_{NW} are the energies of the graphite-supported wire, the bare graphite, and the bare wire, respectively, and m is the number of wire atoms. Thus, the larger E_b is, the stronger the metal−step bond will be. In order to better distinguish the energetics of diverse configurations at the armchair steps, for the strongly and the weakly adsorbed metal atoms (M_s and M_w) the following binding energies were defined.

$$E_{b1}(M_s) = E_G + E_{NW} - E_{GM_s} \quad (2)$$

$$E_{b1}(M_w) = E_G + E_{NW} - E_{GM_w} \quad (3)$$

$$E_{b2}(M_w) = E_{GM_s} + E_{NW} - E_{GSW} \quad (4)$$

E_G is the energy of the bare graphite step, E_{NW} is the energy of the relaxed isolated wire, E_{GM_s} is the energy of the step with only the strongly adsorbed metal, E_{GM_w} is the energy of the step with only the weakly adsorbed metal, and E_{GSW} is the energy of the whole graphite-supported wire (with both M_s and M_w). Equations 2 and 3 correspond to the energy gain of taking one atom from the nanowire and binding it to the step at M_s and M_w, respectively. Equation 4 is the energy gain of taking one atom from the nanowire and binding it to a step in which M_s is already adsorbed. All these binding energies are given in Table 2.

Table 2. Binding Energies, E_b (in eV), of Zigzag and Armchair GSWs amd Binding Energies of Strongly and Weakly Adsorbed Species (M_s and M_w, Respectively)

	Ni	Pd	Pt	Cu	Ag	Au
E_b(zz)	3.00	3.29	3.53	2.27	1.72	1.91
E_b(arm)	2.20	2.24	2.29	1.70	1.40	1.98
$E_{b1}(M_s)$	3.30	3.55	3.81	2.77	2.11	2.33
$E_{b1}(M_w)$	2.34	2.56	2.13	1.24	0.68	0.51
$E_{b2}(M_w)$	1.01	0.73	0.78	0.63	0.69	1.53

dx.doi.org/10.1021/jp406361s | J. Phys. Chem. C 2013, 117, 19239−19244

It is clear from Table 2 that the first metal atom to bind to the armchair step is M_s. The corresponding binding energy is even larger than for the zigzag atoms, principally because M_s is bonded to two carbon atoms, while for the zigzag wire each metal atom is bonded to one. In all cases E_{b1} for M_w is smaller than for M_s by more than 1 eV. These differences are due to the fact that the orbitals of M_w do not overlap with those of the carbon edge, while those of M_s do. Actually, M_w bonds only to M_s and not to the carbon edge.

Two clear trends emerge from Table 2: first, the wires supported on zigzag steps are more stable than those supported on armchair steps. This is due to the fact that, after the first adsorption in the armchair step (M_s), the second adsorption (M_w) is very weak (compare $E_{b1}(M_s)$ with $E_{b2}(M_w)$ in Table 2). Although the M_s–step bond is stronger than that of the zigzag supported wire, the wire–step bond is weaker on average. Only in the case of Au, zigzag- and armchair-supported wires have similar binding energies because its $E_{b2}(M_w)$ is large enough. The armchair edge is more stable than the zigzag edge due to a triple covalent bond between the two open edge carbon atoms;[33] this also favors the metal adsorption on the zigzag edge.

The second trend found is that for zigzag and armchair GSWs the binding energy decreases in the order Ni ≈ Pd ≈ Pt > Cu ≈ Ag ≈ Au. This trend is explained by the nature of the chemical wire–step bond. Two states are particularly involved: one is the sp_y^2 of the C_{edge}, and the other one is a d state of the metal. The combination of both results in bonding and antibonding states, as shown in Figure 3. If the antibonding states are occupied (below the Fermi level), the graphite–wire bond becomes weaker, as is the case for the coinage metals.

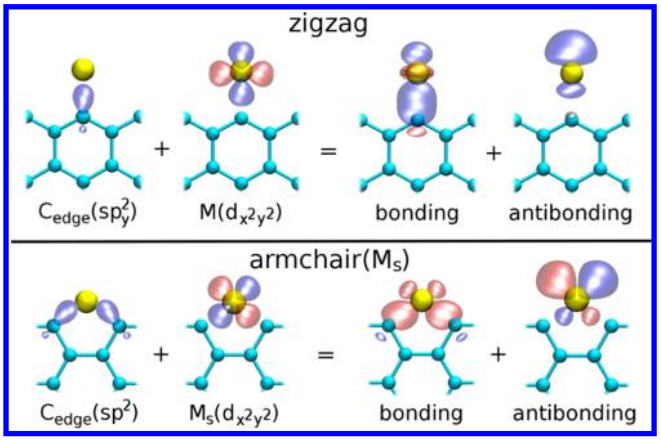

Figure 3. Atomic orbital combination of the graphite wire bond. For the bonding states, the higher probability of finding the electron density is in between C_{edge} and the metal; in the antibonding case, this region is separated by a node.

Figure 4 shows the DOS corresponding to the atomic orbitals shown in Figure 4. The antibonding states are highlighted with arrows.

For zigzag GSWs the antibonding states of Ni, Pd, and Pt are empty, while the antibonding states of Cu, Ag, and Au are filled. This immediately explains why the binding energies are Ni ≈ Pd ≈ Pt > Cu ≈ Ag ≈ Au.

The DOS of the armchair GSWs shown in Figure 4 corresponds to the strongly adsorbed atom, M_s. The positions of the antibonding states are similar to those of the zigzag wires, but in this case Au antibonding states are almost empty. This is

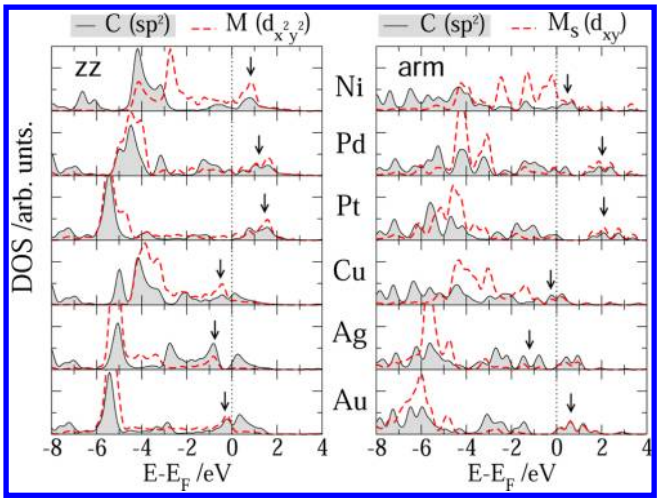

Figure 4. Density of states of the atomic orbitals shown in Figure 3 for zigzag (left) and armchair (right) supported wires. The antibonding states are highlighted with arrows.

in agreement with the binding energies of armchair GSWs since the trend is in the order Ni ≈ Pd ≈ Pt ≈ Au > Cu ≈ Ag.

Hydrogen Affinity. Hydrogen adsorption on GSWs can take place on the metal wire or directly at the edge of the carbon step, which entails the desorption of the wire as shown in Figure 5.

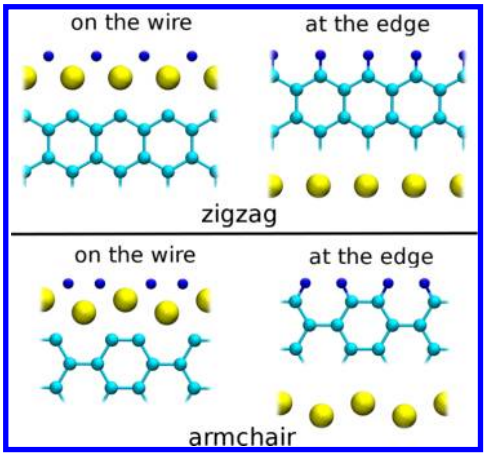

Figure 5. Two possible scenarios for hydrogen adsorption on GSWs for θ = 1 (one hydrogen per metal atom).

In order to compare these two scenarios thermodynamically, the corresponding adsorption energies were calculated. The pertinent reactions are also shown.

$$GSW + H_2 \rightleftharpoons GSWH_2 \quad (5)$$

$$E_{ad}^{wire} = \frac{E_{GSWH_2} - (E_{GSW} + E_{H_2})}{2} \quad (6)$$

$$GSW + H_2 \rightleftharpoons GH_2 + NW \quad (7)$$

$$E_{ad}^{step} = \frac{E_{GH_2} + E_{NW} - (E_{GSW} + E_{H_2})}{2} \quad (8)$$

E_{GSWH} corresponds to the energy of the graphite-supported wire with hydrogen adsorbed, E_{GH} is the energy of a hydrogen-terminated graphite edge, and E_{H_2} is the energy of a hydrogen

dx.doi.org/10.1021/jp406361s | J. Phys. Chem. C 2013, 117, 19239–19244

molecule in a vacuum. Equations 6 and 8 correspond to the adsorption energy per hydrogen atom for a high coverage of hydrogen (one hydrogen per metal atom). Note that both $GSWH_2$ and GH_2 have two hydrogen atoms per unit cell. In order to normalize the energy per hydrogen atom, the equations are divided by a factor of 2. In this case, the more negative the adsorption energy, the stronger is the adsorption. Results are summarized in Table 3.

Table 3. Hydrogen Adsorption Energies (in eV) for High Symmetry Sites of Supported Wires, on the Wire and Directly on the Step Edge,[a] with Values for Hydrogen Adsorption on Freestanding Wires for Comparison

	Ni	Pd	Pt	Cu	Ag	Au
zigzag	*−0.22*	*−0.06*	*−0.29*	−0.18	0.00	−0.26
wire						
C_{edge}	−0.04	0.25	0.48	*−0.78*	*−1.32*	*−1.13*
armchair	*−1.02*	*−0.49*	*−0.78*	−0.73	−0.06	−0.15
wire						
C_{edge}	−0.27	−0.23	−0.22	*−0.78*	*−1.08*	*−0.49*
bare wire	−0.45	−0.75	−0.55	−0.39	0.09	−0.62

[a]The most stable of these two scenarios is highlighted in italics for each metal.

Hydrogen adsorption on Ni, Pd, and Pt supported wires is favored on the wire. On the other hand, for the three coinage metals, hydrogen adsorption is preferred on the graphite step, indicating that for these metals wire desorption is thermodynamically favored. Another clear trend is that hydrogen adsorption is stronger on armchair-supported wires than on zigzag-supported wires, which is in line with the fact that the former are more reactive.

Comparisons with the adsorption of hydrogen on freestanding wires at similar coverages reveal some similarities: The hydrogen−wire bond is stronger for the Ni periodic group than for the Cu periodic group. Of the six metals studied, silver is the worst metal to adsorb hydrogen. Interestingly, the adsorption on nickel and platinum armchair supported wires is even more exothermic than that on their corresponding freestanding wires. Thus, Ni- and Pt-supported wires promise to be good catalysts for hydrogen adsorption, even better than the bare gold wires, but for a definite conclusion it is crucial to calculate reaction barriers, as we shall do in the section Hydrogen Adsorption in an Electrochemical Environment for Pt-supported wires.

Hydrogen Adsorption in an Electrochemical Environment. If we are looking for cheap catalysts, the results of the previous sections are disappointing in comparison with those for freestanding wires.[10] There, we found that the coinage metals Cu and Au were excellent catalysts, while on the supported wire they can be displaced by adsorbed hydrogen, rendering them unstable during hydrogen evolution. At least the transition wires are stable, and it is of interest to compare their activity toward hydrogen with that of the bulk material. We have chosen to investigate platinum as a model substance because of its importance in fuel cell catalysis. Therefore, we have calculated the energy of activation for the adsorption of a hydrogen atom from the solution (Volmer reaction) using the same procedure as for bulk platinum.[34]

Thus, we have calculated the energy of a single hydrogen atom at various distances from the armchair graphite-supported platinum wire; only the distance was kept fixed, otherwise the atom was free to move. These calculations gave us the energy of the atom as a function of the distance, and also its electronic density of states (DOS). From the latter we obtained the constants for the interaction of the hydrogen 1s orbital with the Pt wire, and with these parameters we calculated the free energy surface for the reaction $H^+ + e^- \rightarrow H_{ad}$ as a function of the distance of the reactant from the supported platinum wire and of the solvent coordinate q. For the details we refer to our previous paper[10] (as above).

We remind our readers briefly of the meaning of the solvent coordinate, a concept originally introduced by Hush.[35] During the reaction the configuration of the solvent changes from that appropriate to the solvated proton to that of the adsorbed hydrogen atom. The solvent coordinate q describes the configuration of the solvent during the reaction; we have normalized it in such a way that a solvent characterized by a value q would be in equilibrium with a reactant of charge $-q$.[36]

The corresponding free energy surface is shown in Figure 6 for a potential of 0 V SHE. We have restricted the distance d to

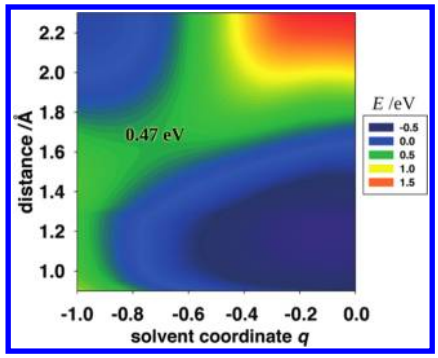

Figure 6. Free energy surface for the adsorption of a proton (Volmer reaction) on an armchair graphite-supported platinum wire as a function of the distance from the electrode and the solvent coordinate q. The calculations have been performed for the equilibrium potential at 0 SHE; all energies are in eV.

the range $d \leq 2$ Å, because at larger distances spin polarization of the hydrogen atom sets in. Far from the wire, centered at $q = -1$, we observe a valley for the solvated proton. The minimum at a distance of $d = 1.1$ Å and $q = 0$ corresponds to the adsorbed hydrogen atom. The two regions are separated by a saddle point with an energy of activation of the order of 0.47 eV, which is somewhat higher than the value of 0.3 eV we observed for a Pt(111) electrode using the same procedure. The difference is caused by the fact that the interaction between the Pt wire and the hydrogen 1s orbital decays more rapidly with distance than at the bulk electrode. The same effect had been observed before for the freestanding wire; it is mainly caused by the different geometry.[37]

■ CONCLUSIONS

In a previous work, it was shown that freestanding nanowires of Cu and Au are excellent catalysts for the hydrogen evolution reaction (HER).[10] Here, we explore the energetics and the catalytic properties of structures closer in their design to that of real devices: metal nanowires supported on graphite/graphene edges. We have examined the energetics of wire formation for several metals at the two most stable graphite edges: zigzag and armchair steps. The binding energy between the step and the metal was found to decrease in the order Ni ≈ Pd ≈ Pt > Cu ≈ Ag ≈ Au. Wires of Ni, Pd, and Pt are more stable due to unfilled antibonding states, which are occupied in the case of

coinage metal wires. In general, wires supported on zigzag steps are more stable than those supported on armchair steps because in the latter case half of the wire atoms are weakly adsorbed to the edge. This entails that supported wires on armchair steps are more reactive toward hydrogen adsorption. In comparison with freestanding nanowires, hydrogen adsorption is in some cases favored at the supported wires (such as Pt supported wires on armchair steps), and in other cases it is favored at bare wires (such as Au freestanding wires). However, the dissociation of molecular hydrogen is exothermic at most supported wires. Unfortunately, the reaction is even more exothermic at the graphite step for the three coinage metals. Therefore, the promising catalytic properties of Cu and Au nanowires are not such at graphite-supported media. Platinum armchair supported nanowires are good catalysts for the hydrogen evolution reaction, but not as good as platinum bulk (111) due to the faster decrease of the metal−hydrogen interaction (coupling constant) for the nanowires. In future studies we will address these topics including other possible structures at the early stages of nucleation, such as oxygen coadsorbed structures.

COMPUTATIONAL DETAILS

First-Principles Calculations. All calculations were performed with DACAPO,[38] a density functional theory (DFT) code. The electron−ion interactions were accounted through ultrasoft pseudopotentials,[39] while the valence electrons were treated within the generalized gradient approximation (GGA) in the version of Perdew, Burke, and Ernzerhof (PBE).[40] An energy cutoff of 450 eV was used with a $(16 \times 1 \times 1)$ k-points Monkhorst−Pack grid[41] for the graphite-supported wires and $(24 \times 1 \times 1)$ k-points for the bare wires. In any case, the increase by 1 k-point, or by 50 eV in the energy cutoff, led to a negligible change in energy of 5 meV. For the relaxations the convergence criterion was achieved when the total forces were less than 10 meV/Å. The orbitals shown have been obtained with the Wannier formalism.[42]

Modeling. GSWs are represented by two graphite layers, one graphite step, and the metal wire as shown in Figure 1. The interplane distance corresponds to that of the experimental systems (3.35 Å).[43] The first two layers act as a supporting media for the step. The surface extends in the xy plane and the edges of the step along the x axis. One side of the step is closed with hydrogen atoms and the other is closed with the metal wire. The step extension along the y axis was optimized by increasing the number of carbon atoms at the step until the change in the wire−step binding energy was less than 40 meV. The convergence was reached with 12 carbon atoms per step for all the metals studied here and for both configurations zigzag and armchair. The steps *gap* (y axis distance between steps) is sufficiently large to avoid the interaction of the step images (10.65 Å for zigzag and 7.37 Å for armchair). The vacuum between surfaces (along the z axis) corresponds to three graphite interplane distances.

The bare graphite substrate (G) is just like the corresponding GSW without the wire. Bare wires (NW) are infinite freestanding one-atom-thick wires along the x axis separated by 12 Å from each other in y and z axes.

The two bottom layers of GSWs and G's were kept fixed and the rest was fully relaxed (including systems with hydrogen absorbed at the wire or at graphite of GSWs, described above). NWs were relaxed in the x axis only.

Ni and Pd bare nanowires were found to be spin polarized with magnetic moments of 1.15 and 0.54 bohr magneton (μB) per atom, respectively. The energy difference with respect to the nonmagnetic systems ($\Delta E_{spin} = E_{spinON} - E_{spinOFF}$) is −0.15 eV for Ni and −0.02 eV for Pd. However, the spin polarization is lost for Pd GSWs and becomes weaker for Ni armchair GSWs, where the magnetic moment is 0.30 μB and ΔE_{spin} = −0.01 eV. The rest of the systems studied do not show magnetic behavior.

AUTHOR INFORMATION

Corresponding Author

*E-mail: german.soldano@uni-ulm.de.

Present Address

[‖]G.J.S.: INFIQC, Departamento de Matemática y Física, UNC, 5000 Córdoba, Argentina.

Notes

The authors declare no competing financial interest.

ACKNOWLEDGMENTS

Financial support by the Deutsche Forschungsgemeinschaft under FOR1376, Mincyt-DAAD, PIP-CONICET 112-201001-00411, and a generous grant of computing time from the Baden-Württemberg grid are gratefully acknowledged.

REFERENCES

(1) Bogozi, A.; Lam, O.; He, H.; Li, C.; Tao, N. J.; Nagahara, L. A.; Amlani, I.; Tsui, R. Molecular Adsorption onto Metallic Quantum Wires. *J. Am. Chem. Soc.* **2001**, *123*, 4585−4590.

(2) Li, C. Z.; Sha, H.; Tao, N. J. Adsorbate Effect on Conductance Quantization in Metallic Nanowires. *Phys. Rev. B* **1998**, *58*, 6775−6778.

(3) He, H. X.; Shu, C.; Li, C. Z.; Tao, N. J. Adsorbate Effect on the Mechanical Stability of Atomically Thin Metallic Wires. *J. Electroanal. Chem.* **2002**, *522*, 26−32.

(4) Kiguchi, M.; Djukic, D.; van Ruitenbeek, J. M. The Effect of Bonding of a CO Molecule on the Conductance of Atomic Metal Wires. *Nanotechnology* **2007**, *18*, 035205.

(5) Castle, P. J.; Bohn, P. W. Interfacial Scattering at Electrochemically Fabricated Atom-Scale Junctions between Thin Gold Film Electrodes in a Microfluidic Channel. *Anal. Chem.* **2005**, *77*, 243−249.

(6) Murray, B. J.; Newberg, J. T.; Walter, E. C.; Li, Q.; Hemminger, J. C.; Penner, R. M. Reversible Resistance Modulation in Mesoscopic Silver Wires Induced by Exposure to Amine Vapor. *Anal. Chem.* **2005**, *77*, 5205−5214.

(7) Hu, J.; Odom, T. W.; Lieber, C. M. Chemistry and Physics in One Dimension: Synthesis and Properties of Nanowires and Nanotubes. *Acc. Chem. Res.* **1999**, *32*, 435−445.

(8) Hammer, B.; Nørskov, J. K. Electronic Factors Determining the Reactivity of Metal Surfaces. *Surf. Sci.* **1995**, *343*, 211−220.

(9) Hammer, B.; Nørskov, J. K. Why Gold Is the Noblest of All the Metals. *Nature* **1995**, *376*, 238−240.

(10) Santos, E.; Quaino, P.; Soldano, G.; Schmickler, W. Electrochemical Reactivity and Fractional Conductance of Nanowires. *Electrochem. Commun.* **2009**, *11*, 1764−1767.

(11) Walter, E. C.; Murray, B. J.; Favier, F.; Kaltenpoth, G.; Grunze, M.; Penner, R. M. Noble and Coinage Metal Nanowires by Electrochemical Step Edge Decoration. *J. Phys. Chem. B* **2002**, *106*, 11407−11411.

(12) Cross, C. E.; Hemminger, J. C.; Penner, R. M. Physical Vapor Deposition of One-Dimensional Nanoparticle Arrays on Graphite: Seeding the Electrodeposition of Gold Nanowires. *Langmuir* **2007**, *23*, 10372−10379.

(13) Quaino, P. M.; Gennero de Chialvo, M. R.; Vela, M. E.; Salvarezza, R. C. Self-Assembly of Platinum Nanowires on HOPG. *J. Argent. Chem. Soc.* **2005**, *93* (4/6), 215−224.

(14) Han, M. Y.; Özyilmaz, B.; Zhang, Y.; Kim, P. Energy Band-Gap Engineering of Graphene Nanoribbons. *Phys. Rev. Lett.* **2007**, *98*, 206805.
(15) Chen, Z.; Lin, Y.-M.; Rooks, M. J.; Avouris, P. Graphene Nano-ribbon Electronics. *Phys. E (Amsterdam, Neth.)* **2007**, *40*, 228−232.
(16) Tapaszto, L.; Dobrik, G.; Lambin, P.; Biro, L. P. Tailoring the Atomic Structure of Graphene Nanoribbons by Scanning Tunnelling Microscope Lithography. *Nat. Nanotechnol.* **2008**, *3*, 397−401.
(17) Nemes-Incze, P.; Magda, G.; Kamarás, K.; Biró, L. Crystallographically Selective Nanopatterning of Graphene on SiO_2. *Nano Res.* **2010**, *3*, 110−116.
(18) Li, X.; Wang, X.; Zhang, L.; Lee, S.; Dai, H. Chemically Derived, Ultrasmooth Graphene Nanoribbon Semiconductors. *Science* **2008**, *319*, 1229−1232.
(19) Wang, X.; Ouyang, Y.; Li, X.; Wang, H.; Guo, J.; Dai, H. Room-Temperature All-Semiconducting Sub-10-nm Graphene Nanoribbon Field-Effect Transistors. *Phys. Rev. Lett.* **2008**, *100*, 206803.
(20) Datta, S. S.; Strachan, D. R.; Khamis, S. M.; Johnson, A. T. C. Crystallographic Etching of Few-Layer Graphene. *Nano Lett.* **2008**, *8*, 1912−1915.
(21) Ci, L.; Xu, Z.; Wang, L.; Gao, W.; Ding, F.; Kelly, K.; Yakobson, B.; Ajayan, P. Controlled Nanocutting of Graphene. *Nano Res.* **2008**, *1*, 116−122.
(22) Kosynkin, D. V.; Higginbotham, A. L.; Sinitskii, A.; Lomeda, J. R.; Dimiev, A.; Price, B. K.; Tour, J. M. Longitudinal Unzipping of Carbon Nanotubes to Form Graphene Nanoribbons. *Nature* **2009**, *458*, 872−876.
(23) Jiao, L.; Zhang, L.; Wang, X.; Diankov, G.; Dai, H. Narrow Graphene Nanoribbons from Carbon Nanotubes. *Nature* **2009**, *458*, 877−880.
(24) Jiao, L.; Wang, X.; Diankov, G.; Wang, H.; Dai, H. Facile Synthesis of High-Quality Graphene Nanoribbons. *Nat. Nanotechnol.* **2010**, *5*, 321−325.
(25) Campos, L. C.; Manfrinato, V. R.; Sanchez-Yamagishi, J. D.; Kong, J.; Jarillo-Herrero, P. Anisotropic Etching and Nanoribbon Formation in Single-Layer Graphene. *Nano Lett.* **2009**, *9*, 2600−2604.
(26) Kuzmenko, A. B.; van Heumen, E.; Carbone, F.; van der Marel, D. Universal Optical Conductance of Graphite. *Phys. Rev. Lett.* **2008**, *100*, 117401.
(27) Balandin, A. A.; Ghosh, S.; Bao, W.; Calizo, I.; Teweldebrhan, D.; Miao, F.; Lau, C. N. Superior Thermal Conductivity of Single-Layer Graphene. *Nano Lett.* **2008**, *8*, 902−907.
(28) Lee, C.; Wei, X.; Kysar, J. W.; Hone, J. Measurement of the Elastic Properties and Intrinsic Strength of Monolayer Graphene. *Science* **2008**, *321*, 385−388.
(29) Acik, M.; Chabal, Y. J. Nature of Graphene Edges: A Review. *Jpn. J. Appl. Phys.* **2011**, *50*, 070101.
(30) Wang, X.; Tabakman, S. M.; Dai, H. Atomic Layer Deposition of Metal Oxides on Pristine and Functionalized Graphene. *J. Am. Chem. Soc.* **2008**, *130*, 8152−8153.
(31) Wang, H.; Feng, Q.; Cheng, Y.; Yao, Y.; Wang, Q.; Li, K.; Schwingenschlögl, U.; Zhang, X. X.; Yang, W. Atomic Bonding between Metal and Graphene. *J. Phys. Chem. C* **2013**, *117*, 4632−4638.
(32) Soldano, G. J.; Quaino, P.; Santos, E.; Schmickler, W. Stability of Gold and Platinum Nanowires on Graphite Edges. *ChemPhysChem* **2010**, *11*, 2361−2366.
(33) Xu, K.; Ye, P. D. Theoretical Study of Atomic Layer Deposition Reaction Mechanism and Kinetics for Aluminum Oxide Formation at Graphene Nanoribbon Open Edges. *J. Phys. Chem. C* **2010**, *114*, 10505−10511.
(34) Santos, E.; Lundin, A.; Pötting, K.; Quaino, P.; Schmickler, W. Model for the Electrocatalysis of Hydrogen Evolution. *Phys. Rev. B* **2009**, *79*, 235436.
(35) Hush, N. S. Adiabatic Rate Processes at Electrodes. I. Energy-Charge Relationships. *J. Chem. Phys.* **1958**, *28*, 962−972.
(36) Schmickler, W.; Santos, E. *Interfacial Electrochemistry*, 2nd ed.; Springer Verlag: Berlin, 2010.
(37) Nazmutdinov, R. R.; Bronshtein, M. D.; Berezin, A. S.; Soldano, G.; Schmickler, W. Bond Breaking Electron Transfer Across a Conducting Nanowire (Nanotube)/Electrolyte Solution Interface: The Role of Electrical Double Layer Effects. *J. Electroanal. Chem.* **2011**, *660*, 309−313.
(38) Hammer, B.; Hansen, L. B.; Nørskov, J. K. Improved Adsorption Energetics within Density-Functional Theory Using Revised Perdew-Burke-Ernzerhof Functionals. *Phys. Rev. B* **1999**, *59*, 7413−7421.
(39) Vanderbilt, D. Soft Self-Consistent Pseudopotentials in a Generalized Eigenvalue Formalism. *Phys. Rev. B* **1990**, *41*, 7892−7895.
(40) Perdew, J. P.; Burke, K.; Ernzerhof, M. Generalized Gradient Approximation Made Simple. *Phys. Rev. Lett.* **1996**, *77*, 3865−3868.
(41) Monkhorst, J. H.; Pack, D. J. Special Points for Brillouin-Zone Integrations. *Phys. Rev. B* **1976**, *13*, 5188−5192.
(42) Thygesen, K. S.; Hansen, L. B.; Jacobsen, K. W. Partly Occupied Wannier Functions. *Phys. Rev. Lett.* **2005**, *94*, 026405.
(43) Baskin, Y.; Meyer, L. Lattice Constants of Graphite at Low Temperatures. *Phys. Rev.* **1955**, *100*, 544.